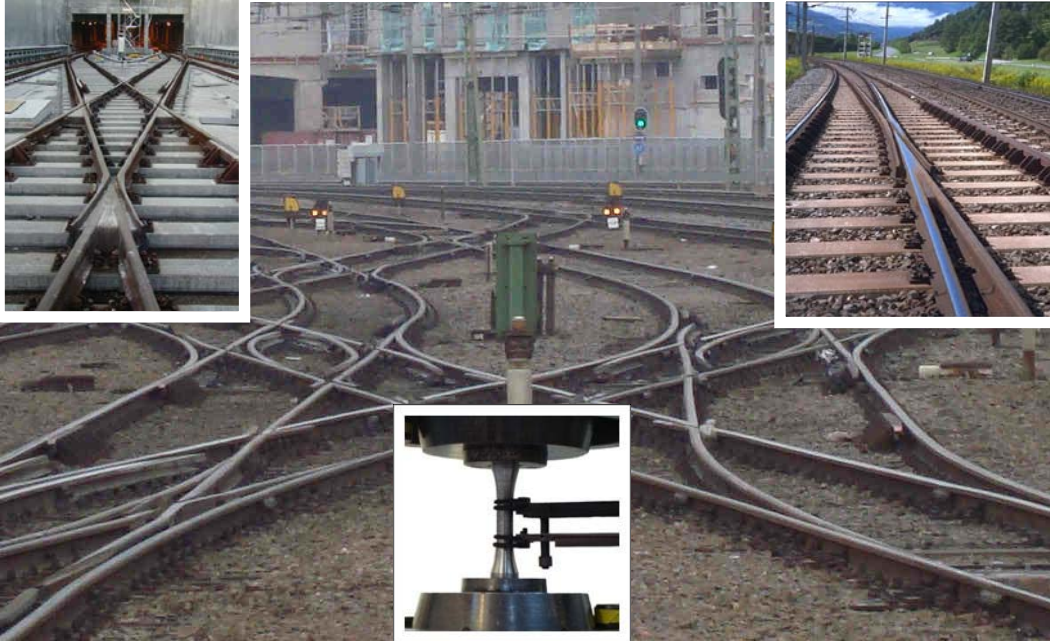


# CHALMERS



## Fatigue properties of austenitic Mn-steel in explosion depth hardened condition

Material used in highly stressed railway components

**Diploma Work in the Master Programme**

**Advanced Engineering Materials**

**LINDA NORBERG**

Department of Materials and Manufacturing Technology

CHALMERS UNIVERSITY OF TECHNOLOGY

Gothenburg, Sweden, 2010

Master Thesis 33/2010

# **Fatigue Properties of austenitic Mn-steel in explosion depth hardened condition**

Material used in highly stressed railway components

by

LINDA M. E. NORBERG

**Diploma work No. 33/2010**

at Department of Materials and Manufacturing Technology  
CHALMERS UNIVERSITY OF TECHNOLOGY  
Gothenburg, Sweden

Diploma work in the Master programme Advanced Engineering Materials

**Performed at:** Department of Materials and Manufacturing Technology  
Chalmers University of Technology, SE - 412 96 Gothenburg

**Supervisor:** MSc. Martin Schilke, PhD-student  
Department of Materials and Manufacturing Technology  
Chalmers University of Technology, SE - 412 96 Gothenburg

**Examiner:** Docent Johan Ahlström  
Department of Materials and Manufacturing Technology  
Chalmers University of Technology, SE - 412 96 Gothenburg

**Fatigue Properties of austenitic Mn-steel in explosion depth hardened condition**

Material used in highly stressed railway components

LINDA M. E. NORBERG

© LINDA M. E. NORBERG, 2010.

Diploma work no 33/2010

Department of Materials and Manufacturing Technology

Chalmers University of Technology

SE-412 96 Gothenburg

Sweden

Telephone + 46 (0)31-772 1000

Cover:

Railway crossings and turnouts, and a specimen during a tensile test.

Chalmers Reproservice

Gothenburg, Sweden 2010

## **Fatigue Properties of austenitic Mn-steel in explosion depth hardened condition**

Material used in highly stressed railway components

LINDA M. E. NORBERG

Department of Materials and Manufacturing Technology

Chalmers University of Technology

## **Abstract**

Railway rails, including crossings and turnouts, are exposed to high impact loads during use and have to resist large cyclic stresses. An extended life time of the railway rails is desired. The high cyclic loads could cause material fracture and a catastrophic failure can occur.

The material studied in this master thesis is cast austenitic manganese steel - Mn13, Explosion Depth Hardened - EDH. Due to the high wear resistance and hardening during use the material can be applied in railway components. The project was cooperation between Chalmers University of Technology and the Austrian company VAE GmbH. The Mn13 EDH steel investigated was the third material in the MU16 CHARMEC-project. The specimens were provided by VAE GmbH.

Tensile, fatigue and hardness tests were performed to examine the mechanical properties and the microstructure of the Mn13-steel was characterised using optical microscopy. Tensile testing was done at three different temperatures (+20°C, +100°C and -60°C) and with two different strain rates ( $10^{-4}\text{s}^{-1}$  and  $10^{-1}\text{s}^{-1}$ ) to determine the effects of deformation speed and temperature. The higher strain rate mainly showed a larger resistance to plastic deformation until failure. The different temperatures had a small influence on the final mechanical properties. Low cycle fatigue testing – LCF was used for performing cyclic uniaxial push-pull tests. The fatigue testing was controlled either by constant strain or stress amplitudes at room temperature. The strain controlled amplitudes were 0.3, 0.4, 0.6 and 1% and the larger amplitudes resulted in the largest plastic strains. Due to small defects in the material, the number of cycles to failure in fatigue testing scattered.

Keywords:

Manganese steel, Hadfield steel, Railway turnouts, Low cycle fatigue, Explosion depth hardening

## **Fatigue Properties of austenitic Mn-steel in explosion depth hardened condition**

Material used in highly stressed railway components

LINDA M. E. NORBERG

Department of Materials and Manufacturing Technology

Chalmers University of Technology

## **Sammanfattning (Swedish)**

Järnvägsräls, inklusive korsningar och växlar, utsätts ständigt för höga utmattningslast och bör därför kunna motstå höga cykliska belastningar. En lång livslängd på järnvägsräl är önskvärd, men de höga cykliska belastningarna gör att det kan bildas sprickor, vilket i sin tur kan leda till brott i materialet. Om en järnvägsräl går sönder, kan detta få katastrofala effekter.

Materialet som undersökts i detta examensarbete är ett gjutet explosionshärdat austenitiskt manganstål, Mn13 EDH. Materialet kan användas till järnvägskomponenter såsom växlar, tack vare materialets goda slitageegenskaper och dess hårdnande under användning. Detta är det tredje materialet som undersökts i projektet CHARMEC - MU16 vilket är ett samarbete mellan Chalmers Tekniska Högskola och ett österrikiskt företag vid namn VAE GmbH. Provtavarna tillhandahölls av VAE GmbH i Österrike.

Drag-, utmattnings- och hårdhetstester gjordes för att kunna definiera materialets mekaniska egenskaper och mikrostrukturen undersöktes med optiskt mikroskop. Dragprovning gjordes vid tre olika temperaturer (+20°C, +100°C och -60°C) med två olika töjningshastigheter ( $10^{-4}\text{s}^{-1}$  och  $10^{-1}\text{s}^{-1}$ ) för att bestämma inverkan av deformationshastighet och temperatur. Högre töjningshastighet gav i de flesta fall större plastisk deformation före brott. Temperaturen hade inte så stor effekt på de mekaniska egenskaperna. Utmattningsprover utfördes i rumstemperatur med konstanta cykliska töjnings- eller lastamplituder. Töjningsamplituderna var 0.3, 0.4, 0.6 och 1 %, där de högsta amplituderna gav den högsta graden av deformation i materialet. Små defekter såsom porer i materialet gjorde att antalet cykler till brott skiljde mycket mellan olika prover.

Nyckelord:

Manganstål, Hadfield stål, Järnvägsväxlar, Lågcykelutmattning och Explosionshårdning

## Acknowledgement

This master thesis was done at the end of the Master programme Advanced Engineering Materials at the Department of Materials and Manufacturing Technology at Chalmers University of Technology, Gothenburg.

The thesis was performed between January to August 2010.

First I want to thank my supervisor **MSc Martin Schilke** for all the support, tutorial, help and introduction with the working equipment during the whole thesis. It was extra nice to be introduced the first week with two conference days and Charmec-meeting.

Furthermore I am thankful to my examiner **Docent Johan Ahlström** for helping me with advice and guidance, especially due to problems with the fatigue testing and Matlab-programming.

I want to give my thankfulness to **Sandra Arvidsson** at department of Materials and Manufacturing Technology at Chalmers University of Technology, for all the administration help, which was used for a confused master student (printing of papers for example...).

I also want to give a extra thought to **Kenneth Hamberg** for help with penetrant testing, **Lars Hammar** for radiography - X-ray of the samples, **Anders Telder** for sample drawings, **Olle Clevfors** for aligning of the testing machine, **Erich Scheschy** and **VAE** for producing of the specimens.

To my opponent **Monika Alander** I want to give a star in the sky, for reading the thesis and supporting me during the whole student time at Chalmers.

Thanks also to my second opponent **Zoreh Ghorbani Tari** for reading and going through the thesis.

Gothenburg August 2010  
Linda Norberg

## **Abbreviations**

Mn13 – the austenitic manganese steel used in this thesis.

EDH – Explosion depth hardening

YS – Yield strength

UTS – Ultimate tensile strength

X-ray – radiography – electromagnetic radiation

R<sub>p0.2</sub> – offset yield strength

LCF – low cycle fatigue testing

## Table of contents

Abstract	
Sammanfattning	
Acknowledgement	
Abbreviations	
<b>1. Introduction</b>	<b>1</b>
1.1 Background	1
1.2 Aims	1
1.3 Limitations	1
<b>2. Railway settings</b>	<b>2</b>
2.1 Turnouts/Crossings	2
2.2 Requirements for turnouts	2
<b>3. Theory</b>	<b>3</b>
3.1 Properties of the Mn13EDH	3
3.2 Manufacturing method	3
3.3 Explosion depth hardening - EDH	4
3.4 Electro discharge machining - EDM	4
3.5 Radiography – X-ray	5
3.6 Penetrant testing	5
3.7 Tensile testing	5
3.8 Fatigue testing	7
Low cycle fatigue testing - LCF	8
Strain controlled	8
Stress controlled	8
3.9 Hardness testing	9
Vickers	9
<b>4. Experimental part</b>	<b>10</b>
4.1 Test specimens for tensile and fatigue testing	10
4.2 Manufacturing of the samples	10
4.3 X-ray testing	11
4.4 Preparation of samples	11
4.5 Microstructure	11
4.6 Hardness testing	12
4.7 Tensile and fatigue machine	13
4.8 Tensile testing	14
4.9 Fatigue testing	15
<b>5. Result</b>	<b>16</b>
5.1 Radiography by X-ray	16
5.2 Microstructure	16
5.3 Hardness testing	17
5.4 Tensile testing	19
5.5 Fatigue testing	22
5.6 Fracture surfaces	26
<b>6. Discussion</b>	<b>27</b>
6.1 Radiography	27
6.2 Tensile and fatigue testing	27
<b>7. Conclusions</b>	<b>28</b>
<b>References</b>	<b>29</b>
<b>Appendix 1</b>	<b>30</b>

## 1. Introduction

### 1.1 Background

This master thesis was done in cooperation between Chalmers University of Technology and the Austrian company VAE GmbH (owned by Voestalpine AG). VAE mainly work with materials for railway turnout and crossing technology. The material investigated in the current project was a cast austenitic manganese-steel - Mn13, hardened by explosion depth hardening- EDH. It was also the third material studied within the MU16 CHARMEC-project. The two other earlier investigated materials were a cast austenitic Mn13-steel, without any following hardening and a martensitic steel SAE6150 (DIN51CrV4).

The specimens were provided by VAE GmbH in Austria.

### 1.2 Aims

The main goal for the project was to characterise the mechanical behaviour of austenitic manganese steel – Mn13EDH, used for highly stressed rails in railway turnouts and crossings. The material was investigated through radiography X-ray, penetrant, hardness, tensile and push-pull low cycle fatigue testing. The main attention was on fatigue. The focus point during the testing was to figure out the mechanical properties in the material to have an opportunity to increase the safety, decrease life cycle cost and prolong the lifetime of railway rails.

### 1.3 Limitations

Except for hardness, tensile and fatigue testing, the material through dimensions, casting and manufacturing method were limiting factors. The monotonic tensile testing was performed at different temperatures (+20°C, +100°C and -60°C) and also with different strain rates ( $10^{-1}\text{s}^{-1}$  and  $10^{-4}\text{s}^{-1}$ ). The results of the tensile testing were mechanical properties like yield strength – Y.S, start of plastic deformation - Rp0.2, strain hardening ratio, ultimate tensile strength - UTS and fracture strain.

The low cycle fatigue testing - LCF was performed at room temperature (~20°C). The fatigue tests were either strain- or stress controlled. Strain controlled tests were done at different total strain amplitudes ( $\pm 0.3\%$ ,  $\pm 0.4\%$ ;  $\pm 0.6\%$  and  $\pm 1.0\%$ ), which was kept on a constant level during each fatigue test. The maximum load levels at half of number of cycles to failure ( $N_f/2$ ) under strain controlled testing, were converted to comparable stress amplitudes for stress controlled testing.

To have an opportunity to figure out the reliability of the results, all tests were repeated twice at each level.

## 2. Railway settings

### 2.1 Turnouts/Crossings

When a train or tram wants to change track, turnouts and crossings are used. Another reason for crossings is when two lines cross but such crossings are more frequent used in slower tram traffic. See Figure 1 and Figure 2.



Figure 1. Turnout, most frequent in train operation.  
Courtesy by VAE.



Figure 2. Crossings, more frequent in tram operation.  
Courtesy by VAE.

### 2.2 Requirements for turnouts

The purposes for the turnouts are to give a train or tram opportunity to change track. The turnout has to resist large impact loads since the passing through only is momentary. Increased impact stresses on the blade of the turnouts create deformation in the material and as an effect fatigue cracks can occur.

### 3. Theory

#### 3.1 Properties of the Mn13EDH

The material investigated in the project is an austenitic manganese steel, Mn13-steel, which is hardened by explosion depth hardening - EDH. The material is quite ductile and the Mn steels are also called Hadfield steels, after the discoverer of the material.

The chemical composition of the Mn13-steel can be seen in Table 1.

**Table 1. Chemical composition of Mn13EDH**

Manganese, Mn	Carbon, C	Silicon, Si
13%	1%	0.5%

Manganese -Mn is a stabiliser of austenite, which allows the material to remain in face centered cubic crystal structure – FCC, even at room temperature. With a larger amount of Mn (up to 14%) the tensile strength increases. The large content of Mn also helps the material to combine good wear resistance and work-hardening rate with high toughness. (Lewis & Olofsson, 2009)

The austenitic Mn-steel has high strain hardening (in polycrystalline form), high wear resistance and high toughness. Strain hardening is the dominating hardening mechanism in the material and it is one of the most important properties for Hadfield steel. The material normally hardens during use and can be applied in highly stressed rails and wear applications like turnouts and crossings. The properties of the material mostly depend on how large the mobility of the dislocations are and how the material can handle deformations. (Efstathiou & Sehitoglu, 2009).

#### 3.2 Manufacturing method

The Mn13EDH-steel specimens are cast and the quality of the material will depend on casting method and containing materials. Materials without defects are favourable for low cycle fatigue testing - LCF. It is impossible to produce a cast material without defects and there will always be some defects like pores, slags and inclusions.

To eliminate and reduce gas precipitations (N, O and CO<sub>2</sub>) in the material, aluminium –Al or titanium -Ti can be put in the melt. Through binding there will be a chemical reaction and the result of this is smaller grains and a decrease of grain growth.

### 3.3 Explosion depth hardening - EDH

The material investigated in this thesis is hardened by depth explosion. The plate of Mn-steel is covered with a layer of explosives. The plate is mounted on a fixation box to be fastened during the detonation. On ignition there will be a detonation, causing shock-waves to pass through the plate. This will give the material a larger amount of dislocation density and thus make the material harder. See Figure 3. (Ahlström 2009)

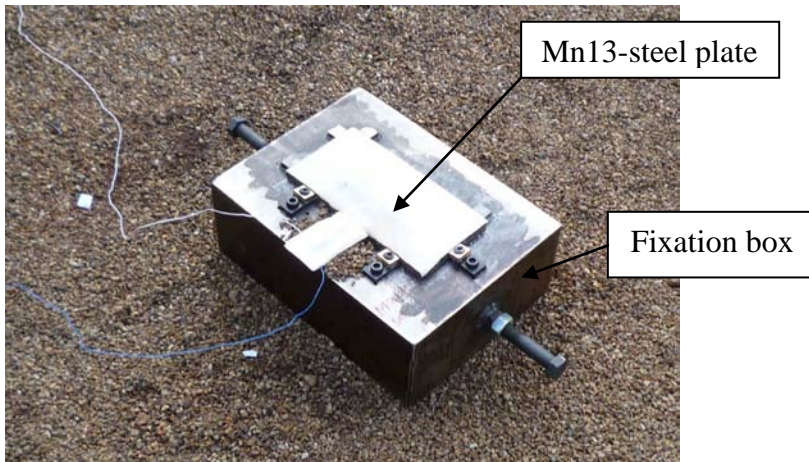


Figure 3. The plate of Mn-steel, hardened by explosion depth hardening. Courtesy by VAE.

### 3.4 Electro discharge machining - EDM

Electro discharge machining - EDM, is a method where electro discharges (equal to sparks) is used and can be called spark or wire erosion. The specimens used in this master thesis were cut out with sparks. See Figure 4.

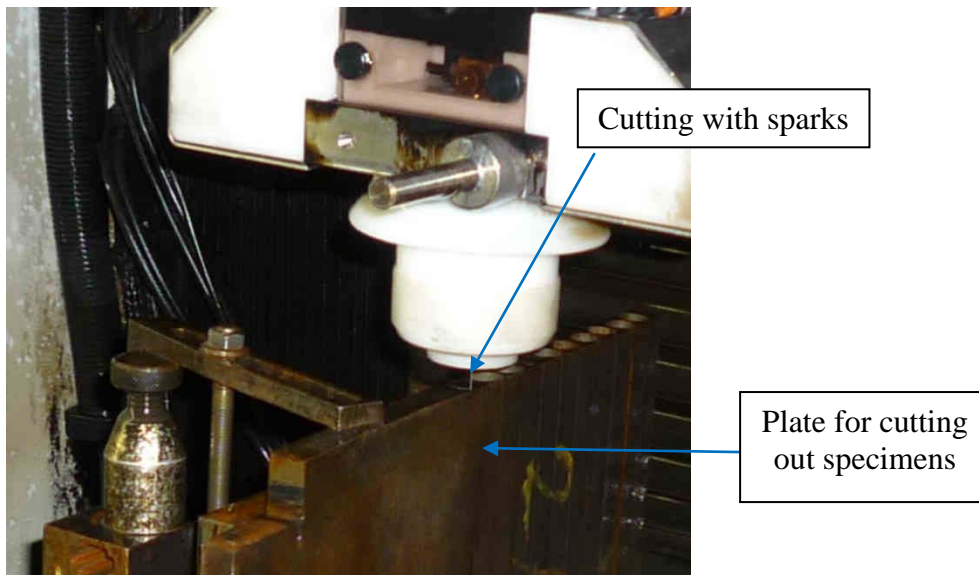


Figure 4. Electro discharge machining. Courtesy by VAE.

### 3.5 Radiography – X-ray

Radiography - X-ray, is a method to recognise impurities like inner defects, inclusions, pores and outer defects on the surface area in the material. When using the X-ray equipment exposures should be done both in parallel and perpendicular direction at the sample to find oriented defects. The result can be captured using a film or a digital device.

### 3.6 Penetrant testing

Penetrant testing is a non-destructive method and can be used to visualise surface defects at the samples. In fatigue testing, surface defects like pores, slags or scratches are often starting points for crack initiation. The sample surfaces were examined with penetrant testing, but as this gave no additional information compared to visual inspection, the results of this study are not further reported.

### 3.7 Tensile testing

Tensile testing is a method, where uniaxial load is used and the material will be stressed under a certain load in tension. The continuously increasing load makes the material go through elastic, plastic and failure part. The material will become permanently plastically extended during the test. The strain,  $\varepsilon$  [%] and stress,  $\sigma$  [MPa] can be used to characterise the properties of a material and is used in a stress-strain curve. See Figure 5. (Dieter, 2003) (Callister, 1997)

*Stress-strain curve*

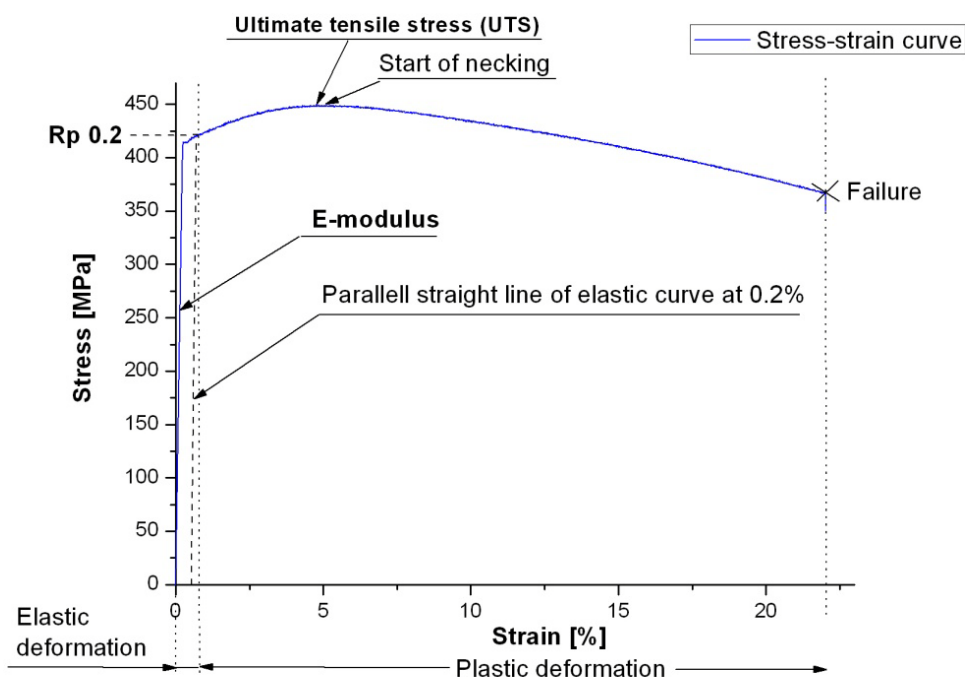


Figure 5. Schematic Stress/strain-curve

*E-modulus/Young's modulus – E*

E-modulus describes the stiffness of the material. A larger value shows better resistance to elastic deformation and when a material undergoes stress, there will be a deformation in the material. Normally a material can undergo two different stages of deformation.

The first one is the linear elastic part, which can be described by Hooke's law.

See Equation 1. (Ullman, 1997)

$$E = \Delta\sigma / \Delta\varepsilon \text{ or } \sigma = E \cdot \varepsilon$$

Equation 1. Hooke's law

$E$  is the elastic modulus also called Young's modulus [GPa] and is the initial slope of the stress-strain curve. If a material will be unloaded in this elastic part of the curve, the material will return to original shape.  $\sigma$  is the applied stress [MPa] and  $\varepsilon$  is the strain in the material [%]. See Figure 5.

Stress and strain is often expressed in curves as engineering stress or strain, where the denomination is due to the use of the initial area of the specimen. A calculation can be done with Equation 2. (Callister, 1997)

$$\sigma = F/A_0$$

Equation 2. Calculating of Engineering Stress

Where  $F$  is the load used,  $A_0$  is the initiation area used when starting the test and  $\sigma$  is the engineering stress. (Callister, 1997)

*Yield strength - YS*

The exact yield strength point, where the material goes from the elastic to plastic part, is hard to define. Therefore a straight line, parallel to the elastic deformation part of the curve, is drawn at value 0.2% strain and the stress when this line intersects the test curve is called  $R_{p0.2}$ . See Figure 5.

In Figure 5, the elastic part of the material shows how much stress the material can withstand without changing structure and deform plastically. If the material will be unloaded in this area the material will return to original shape as said above. Units used for yield strength are [MPa] or [ $N/mm^2$ ].

During the next stage of the curve, there will be a permanent plastic deformation and strain hardening left in the material. The specimen has lost the opportunity to return to original shape. At sufficiently high strains, cracking occurs and the material will fracture.

If the material is deformed and quite soft, ductile and heterogeneous, there will be a localised reduced diameter during tensile testing and it is called necking. See Figure 6.



Figure 6. Necking of a ductile and heterogeneous material

#### *Ultimate tensile strength - UTS*

Ultimate tensile strength, also called tensile strength - TS, is the largest stress value the material can resist. See Figure 5. Units used for UTS: [MPa] or [N/mm<sup>2</sup>].

#### *Fracture strain, the Failure*

Fracture strain is when the material failure and break. Units used for fracture strain is [%]. See Figure 5.

### **3.8 Fatigue testing**

Fatigue is the most common reason for failure and it will come due to cyclic stresses or strains, where the maximum values are less than the static yield strength of the material. The testing is done under an unknown number of cycles to failure. Fatigue can be summarised with localized and permanent damage at a structural level in the material. The fatigue testing shows how good a material can resist cyclic strain or stress before breaking. (Fatigue and Fracture Mechanics, ASM Handbook online vol.8., 2003)

Different materials show different fatigue behaviour, due to production, manufacturing method, heat treatment and heterogeneity of the material. Minimizing of the surface defects and inner irregularities like pores and slags are to be desired, but in cast materials it is more difficult achieving a homogeneous material. Pre-processing or redesigning of a detail can be another way of avoiding of cracking in the material.

### *Low cycle fatigue testing - LCF*

The fatigue testing performed within this thesis is low cyclic fatigue testing -LCF, where high load levels are used, often with stress amplitudes larger than the yield strength. The characteristic of LCF is that the material undergoes a plastic deformation during testing. Compared to tensile testing there is a requirement of both tensile and compressive load to make the material failure. The fatigue test can either be strain- or stress controlled.

In LCF-testing the material undergoes different stages of deformation. First there is an elastic deformation and then a global cyclic plastic deformation and cracking of the material which ends up with a failure. The cracking of the material is often due to some crack initiation points like surface defects or pores. This is the first damage of the material and there will be propagation of the crack. If pores and slags precipitate, the material will have rather bad properties. (Fatigue and Fracture Mechanics, ASM Handbook online vol.8., 2003)

### *Strain controlled*

When having strain controlled test, the sample is pulled until a certain level of strain [%] is reached. The strain amplitude is kept on a constant level during the whole test. The important result in this test is how the stress changes during the testing.

The method is material dependent and the results of the experiment of each sample can be arranged in a Coffin-Manson diagram, where the plastic stress amplitudes are compared to number of cycles to failure,  $N_f$ . The Coffin-Manson diagram shows the plastic strain amplitude ( $\Delta\epsilon_p/2$ ) vs the number of cycles to failure ( $N_f$ ) and is used to evaluate the safe strain amplitude, that can be used considering a certain fatigue life.

### *Stress controlled*

In a stress controlled (or more correctly expressed, load controlled) testing, the test sample is pushed and pulled until a certain level of stress is reached. The stress amplitude is kept constant during the test. The important results in this type of testing are how the strain changes during the test.

The results of a stress controlled test can be arranged in a Wöhler-like diagram, where the interesting outcome of this is the strain amplitude change ( $\Delta\sigma/2$ ) vs. number of cycles ( $N_f$ ). The Wöhler-like diagram expresses the stress life with an S-N-curve, where S is stress and N is number of cycles.

### 3.9 Hardness testing

When hardness testing is performed, there is an indenter pushed into the material with a certain load. At the tested surface there is a small imprint made and it could be measured and transformed to hardness number. During the testing there will be a small indent but there will not be any damage deeper into the material. The choice of indenters varies according to what type of material, method, geometry and microstructure the sample has. The load is based on what information is wanted, type of material and microstructure the sample has.

There are various types of measuring of hardness within different indentations; Brinell indentation is spherical, Rockwell conical, Vickers and Knoop have pyramidal indentation. Rockwell measurement is due to the depth of the indentation but the other methods are measuring the dimensions of the imprint in millimetres. All these methods are static ways of measure the hardness in a material and the unit used is load in kilograms per square millimetre [ $\text{kgf/mm}^2$ ]. (Revanker, 2003), (Edward L. Tobolski, 2003), (George F, 2003), (Ullman, 1997)

Hardness testing is a simple and quite cheap non-destructive method, where the mechanical properties like tensile strength can be estimated after the testing. Hardness testing is used for materials like metals, ceramic and semiconductors, but also softer materials like polymers and elastomers. (Revanker, 2003) (Callister, 1997)

#### *Vickers*

The method used in this master thesis is Vickers and it is commonly used, simple and inexpensive method. The hardness scale of Vickers can be used in all materials, from soft to hard ones and even for carbides. Vickers was introduced first time in England 1925. (Edward L. Tobolski, 2003)

An advantage with Vickers is the use of the magnitude, where it can be used both for micro- and macro hardness. A disadvantage is that the material has to be polished to have a flat surface. Vickers is measured with a pyramidal indentation, where the angle between the edge surfaces is  $136^\circ$ . (Revanker, 2003), (Edward L. Tobolski, 2003), (George F, 2003), (Ullman, 1997)

The experimental part of Vickers method works like this: A sample is placed in the machine and a pyramidal indenter is pushed with a certain load against the surface of the sample. The two diagonals of the pyramidal area is measured with a ruler on a microscopy screen. See Figure 7.

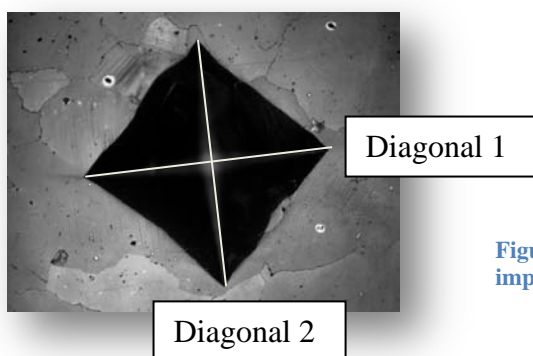


Figure 7. Vickers testing method, measuring of the diagonals of imprint.

An average value of the two diagonals is taken and compared with a table to get a hardness number in unit Hardness Vickers, HV.

## 4. Experimental part

The experimental work with tensile, fatigue and hardness testing was evaluated at the department of Materials and Manufacturing Technology at Chalmers University of Technology in Gothenburg 2010.

### 4.1 Test specimens for tensile and fatigue testing

The specimens were prepared, machined and provided by VAE GmbH in Austria. The cylindrical specimens were used for both tensile and fatigue testing and had dimensions showed at Figure 8.

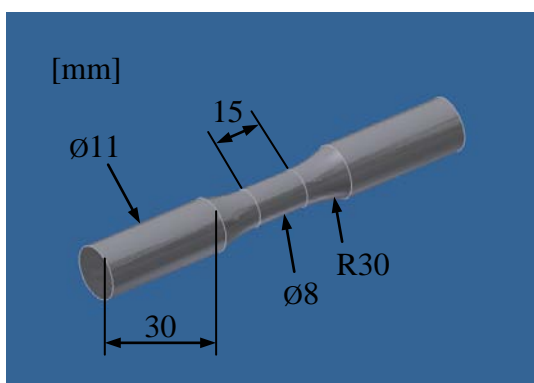


Figure 8. Appearances and dimensions of test samples.

In the as cast Mn13 tested previously within the MU16 CHARMEC project, a gauge diameter of 6 mm was used. For this study, the diameter was increased from 6 mm to 8 mm. The reason of the changed diameter was to avoid buckling during testing. The total length was approximately 100 mm.

### 4.2 Manufacturing of the samples

The preparation and the machining of the samples were completed by VAE in Austria. The cast block was split into two pieces called plate C/D and A/B respectively. Thereafter each plate was hardened by depth explosion from both sides. Samples were cut out by electro discharge machining (18 samples from plate C/D and 13 samples from A/B). See Figure 9A and 9B.



Figure 9A. Samples cut out of plate A/B



Figure 9B. Sample cut out of plate A/B

### **4.3 X-ray testing**

Test bars were examined with radiography prior to mechanical testing in order to find inner defects in the material like pores, slags and inclusions. Tagging of the samples was the first to be done before sending the samples away to the X-ray radiography testing. The samples were marked with a line and photographed from two angles with 90 degrees difference in order to improve detect oriented defects.

The X-ray was performed at Volvo Aero by Lars Hammar. To recognise and see what quality the defects had in the material, there were reference wires put on the samples. A filter was used to smoothen out the differences and the colour measured depends on the line profile.

### **4.4 Preparation of samples**

#### *Grinding and polishing*

Before tensile and fatigue testing the samples were both ground and polished to take away stress concentrations and residual stresses from the manufacturing. The preparation was also made to minimize crack initiation points, like surface defects and sharp edges.

The grinding of the samples was done in steps with slips of a SiC-paper on a turn, where it started with a coarse-grained abrasive paper (120) and ended with the finer one (1200). To avoid unwanted heating and deformation, water was used as lubricant. For fatigue testing the polishing continued in steps with even finer abrasive paper (2400, 4000) and ended up with 7  $\mu\text{m}$  down to 1  $\mu\text{m}$  with diamond paste and ethanol as the lubricant.

#### *Visual inspection*

Cleaning and visual inspection was done after each step of grinding and polishing. The visual inspection was made with an optical light microscopy to see if the scratches from the last polishing step were gone.

### **4.5 Microstructure**

Before the hardness testing the samples were ground and polished in steps with diamond paste from 7 $\mu\text{m}$ , 2.5 $\mu\text{m}$  down to 1.25 $\mu\text{m}$ . Ethanol was used as a lubricant during the polishing.

Etching was made with the chemical liquid Nital (3%) at the polished surface to see the microstructure of the sample. The microstructure was checked in a microscopy to observe types of grains and their size.

#### 4.6 Hardness testing

The specimens used for the two other materials in the MU16-project, had one elongated end of the specimen, where the hardness testing could be made. Unfortunately the specimens used in this thesis did not have any extra elongated material for hardness testing. The testing was instead evaluated at two different special pieces cut from the two plates C/D and A/B.

The hardness testing was performed in a Wolpert machine, where prepared samples were placed on a table. The pyramidal indenter was pushed against the surface with a certain indentation load (30kg) and was held for about 10-15 sec (called dwell-time). The machine had a microscopy screen, where the imprint could be seen. The diagonals of the imprint were measured at the screen (with a magnitude of 500×) with a ruler. See Figure 10.

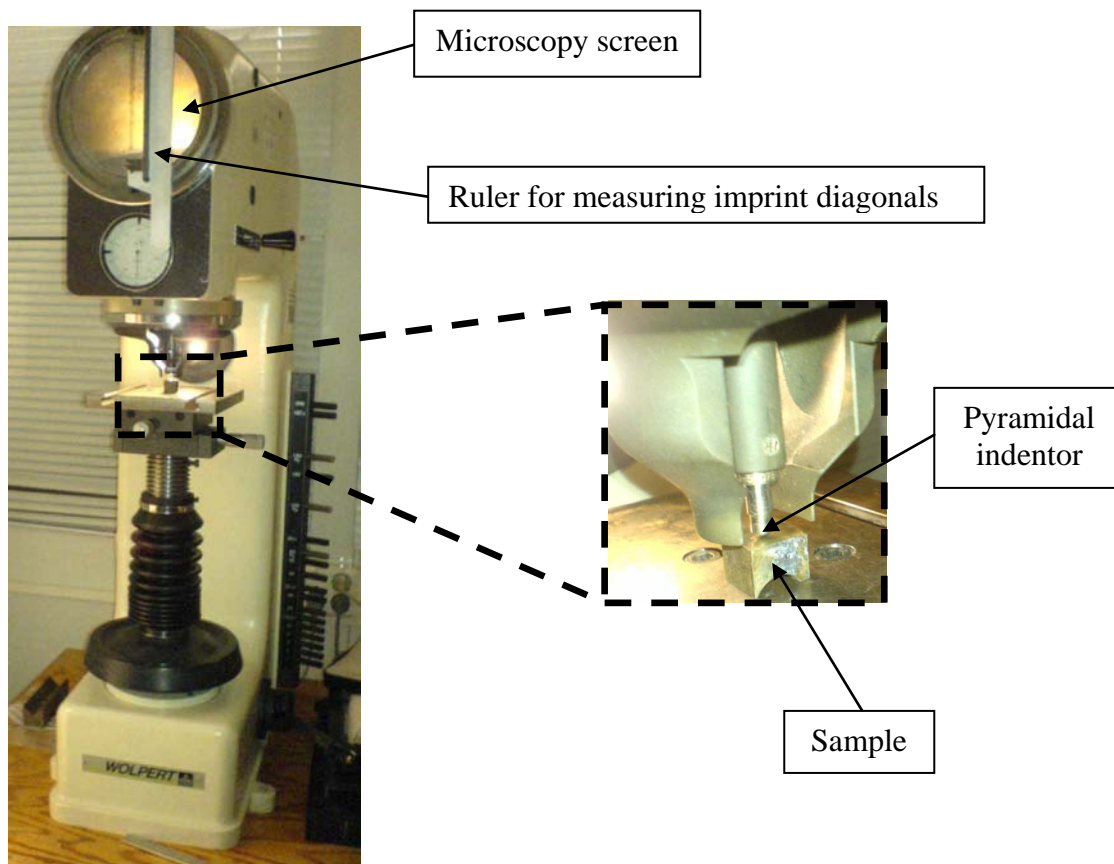


Figure 10. Hardness testing machine, Wolpert probat dia testor 2RC 7021.

Another function of the microscope was to place the indent at a proper position on the sample.

#### 4.7 Tensile and fatigue machine

The Instron 8032 machine is servo-hydraulic, which was both used for tensile and fatigue testing during the thesis. See Figure 11.

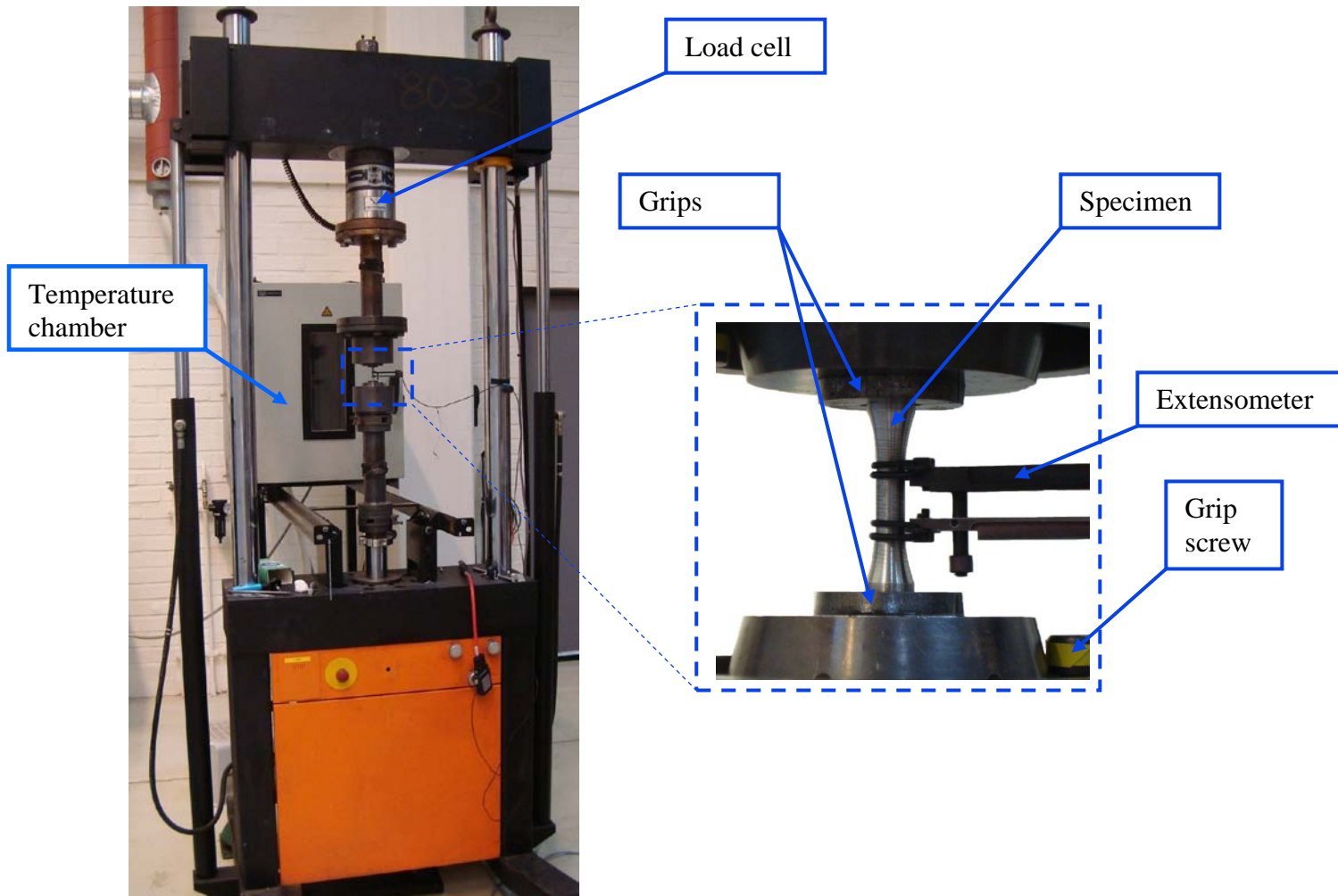


Figure 11. Tensile and fatigue machine, Instron 8032.

Before using the hydraulic Instron 8032 machine and computer equipment both for tensile and fatigue testing, the pump had to be turned on and the process was checked according to instructions done by Martin Schilke and Johan Ahlström.

The actuator was a hydraulic cylinder where the energy comes from an oil pump. When performing tensile testing at lower ( $-60^{\circ}\text{C}$ ) and higher ( $+100^{\circ}\text{C}$ ) temperatures, a temperature chamber was needed. The chamber was removable, controlled electronically and could work in a temperature range from  $-70^{\circ}\text{C}$  to  $+350^{\circ}\text{C}$ . See Figure 11.

### *Sensors for tensile and fatigue testing machine*

1. Linear Variable Displacement Transducer – LVDT, is used for measuring of the position or displacement and for guiding (not used in this thesis).
2. Load cell is used to measure load or force. See Figure 11.
3. Extensometer is used to measure strain. See Figure 11.  
When performing fatigue testing a short leg extensometer, with up to 10% opportunity to elongate was used.

The Instron 8032 had MTS-guiding software where the set values like strain rate, frequency, position, time, strain or stress at each test was introduced. Origin and Matlab was used to evaluate the tests and get graphs and results out of the MTS-software.

### **4.8 Tensile testing**

The tensile testing was executed at three different temperatures (+20°C, +100°C and -60°C) and with two different strain rates ( $10^{-4}\text{s}^{-1}$  and  $10^{-1}\text{s}^{-1}$ ). The parameters were predetermined to see if surrounding environment and speed make some difference at the material behaviour.

When measuring the elongation during the test a long leg extensometer was used, capable of measuring up to 40% elongation. The attachment of the extensometer was made by rubber rings at room temperature and with steel springs when using the higher or lower surrounding temperature. Crochet hooks were used to pull the bands or springs around the samples. The blades of the extensometer had to be sharp to avoid sliding at the sample.

When doing the tensile testing the distance between the mounting grips were quite long. It gave the opportunity to use a mobile temperature chamber, when testing at higher and lower temperature compared to room temperature. The temperature was held constant during the entire testing. When performing the test at lower temperatures, liquid carbon dioxide -  $\text{CO}_2$  was used as a cooling agent.

The testing was executed at samples with a diameter of 8 mm, where two tests were done at each combination of temperature and strain rate.

## 4.9 Fatigue testing

After tensile testing, the machine was rebuilt to have a shorter distance between the grips. The shorter rods were mounted to reduce buckling of the fatigue tested samples. Also aligning and calibration of the machine was completed. As for tensile testing, the specimens had to be clamped into the machine but due to sliding in the grips, the torque at the tightening screws was increased from 25 to 35 Nm.

The extensometer with the short legs was used during the test for measuring of the strain and the limitation level of the elongation was 10%. Rubber rings were used to fasten the extensometer at the samples. The blades of the extensometer have to be sharp to avoid sliding and to secure the perfect contact with the material.

To have a comparable result of the testing, two tests on each level of both strain and stress controlling were run.

Cracks due to fatigue are often initiated at inner defects and since this material had less surface defects than inner defects, the grit grinding was stopped at a level of 1200 instead of mirror-like as the original schedule was. The cause of the grit grinding of the surface is to take away stress concentrations at the material.

The low cycle fatigue testing samples were run in either stress or strain control.

### *Strain controlled*

The predetermined strain levels were 0.4, 0.6 and 1%. Because of troubles with buckling at the level of 1%, there had to be some extra tests done at 0.3%. During testing of the first specimens in strain controlled fatigue at 0.4%, the load became high due to hardening. For the higher strain amplitudes, the diameter of the specimens was therefore reduced from 8 mm to 7 mm, to avoid risk for overloading of the test machine.

### *Stress controlled*

In the stress controlled fatigue tests, there was a calculation from strain levels already measured to corresponding stress levels. The testing was done on samples with a diameter of 8 mm and two tests were done for each stress level.

## 5. Result

### 5.1 Radiography by X-ray

Radiography by X-ray was made at two times during the master thesis on samples taken from plate C/D and A/B. Most of the test bars had no pores larger than 0.3mm. An example of a X-ray image could be seen at Figure 12.

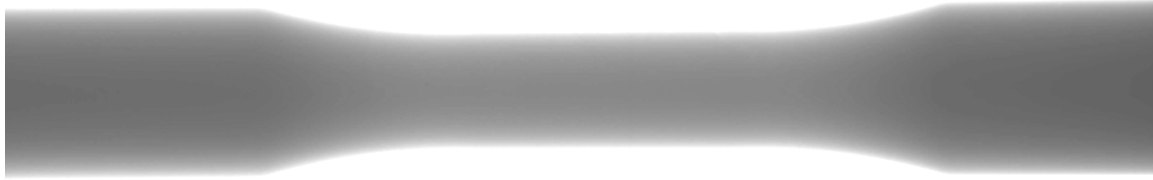


Figure 12. X-ray image of a specimen. Defects cannot be seen at current magnification.

Both inner and surface defects could be seen during X-ray testing. Examples can be seen at Figure 13A, B and C.

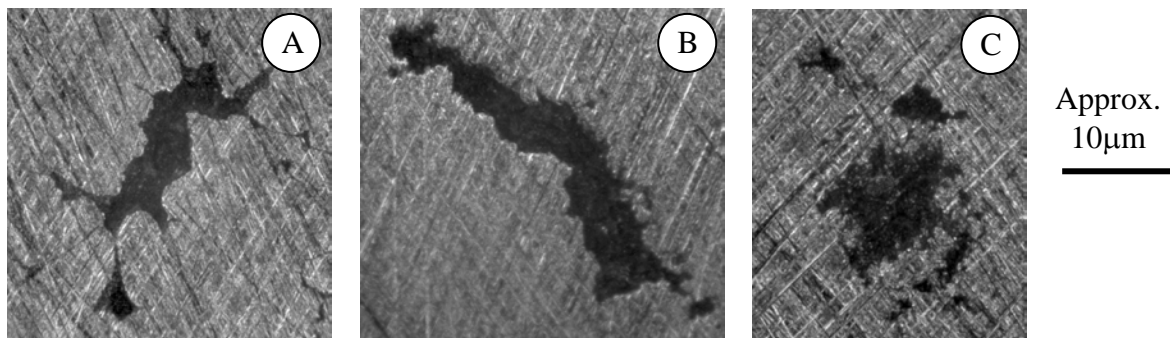


Figure 13. Defects in the material A. Slag B. Slag C. Pore

### 5.2 Microstructure

When looking at the microstructure of the austenitic Mn-steel, there were some quite large black areas that were pores in the material. Small black dots look like carbides. Due to the high amount of Mn in the material, the microstructure can remain austenitic. The size of the grains differs a lot. See Figure 14.

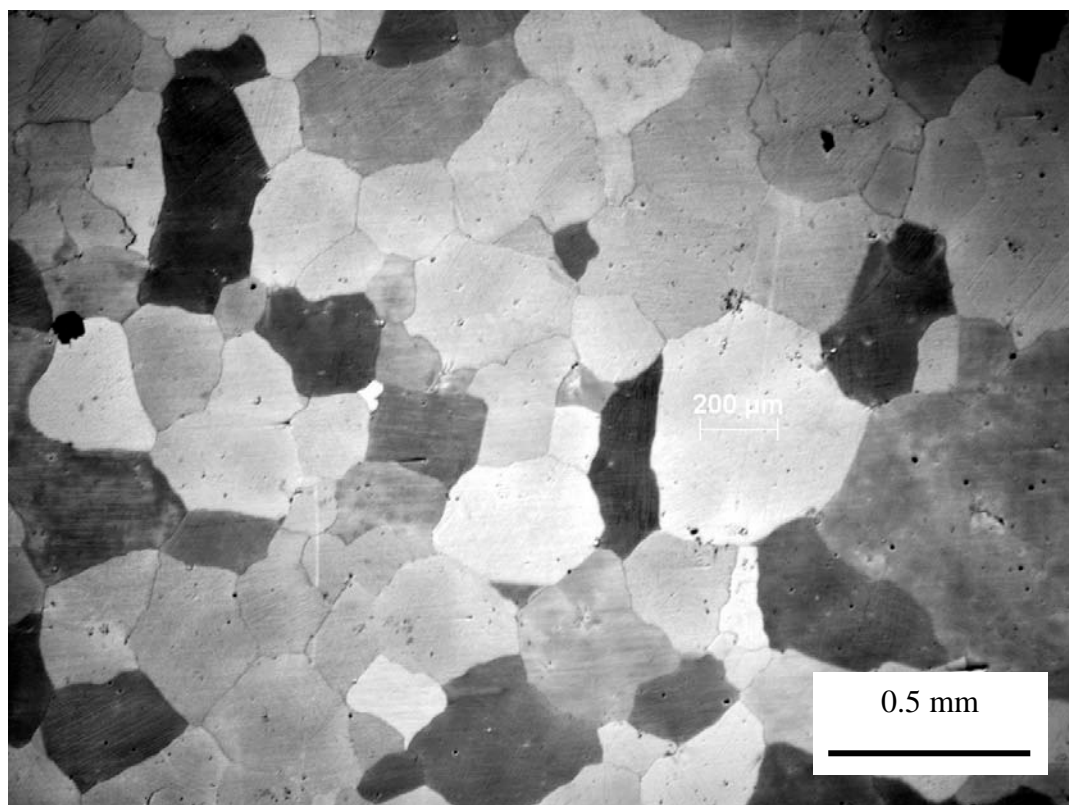


Figure 14. Microstructure of Mn-steel, hardened by explosion depth hardening.

### 5.3 Hardness testing

To get the hardness number in Vickers HV, the average value of the measured diagonals of each indentation was compared to a ASTM table. See table 2.

Table 2. Extract out of ASTM E 92, comparison of average diagonal and hardness number.

Average measured diagonals [mm]	Hardness number [HV]
0.39	366
0.40	348
0.41	331
0.42	315
0.43	301
0.44	287
0.45	275

There have been 18 hardness measurements at a piece cut from plate C/D and it showed an average value of the hardness at approximately 301HV. See Figure 15.

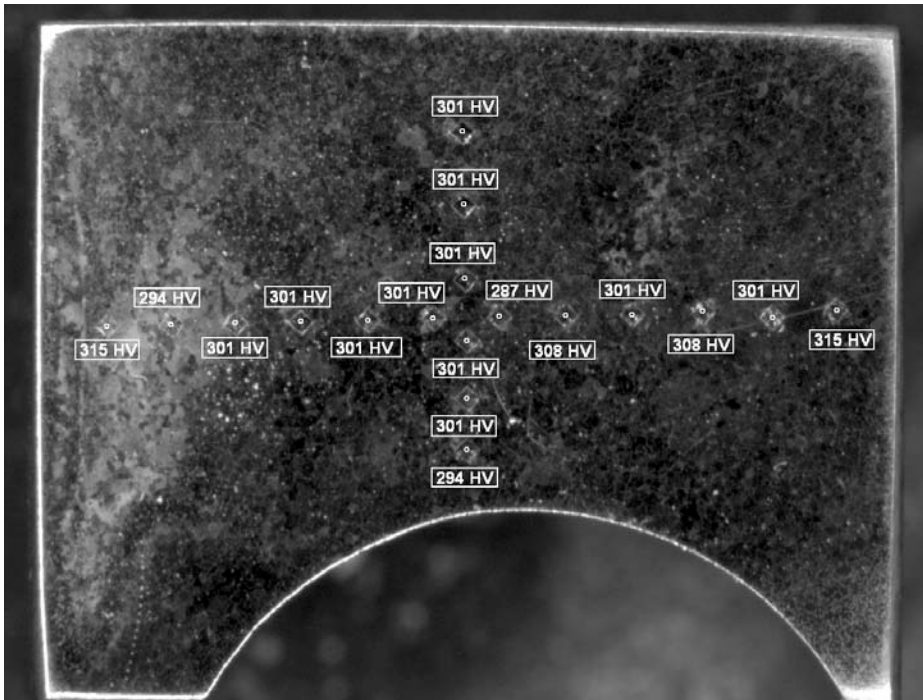


Figure 15. Hardness testing of plate C/D

There have been 16 hardness measurements made on a piece cut out from plate A/B and it showed an average hardness value of approximately 327HV. See Figure 16.

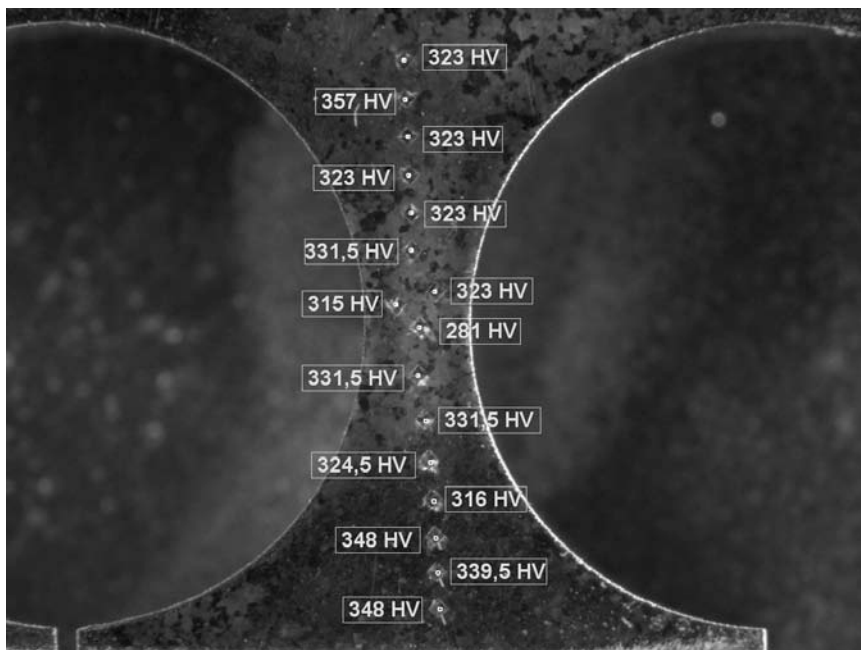


Figure 16. Hardness testing of plate A/B.

The plate A/B had a higher average value of the hardness, but there was a small variation through the thickness in the both plates and a possibly explanation to that could be the explosion depth hardening.

## 5.4 Tensile testing

The tensile testing was performed at three different temperatures with two different strain rates. A comparison between each temperature was made and the results can be seen in Figure 17, 18 and 19.

Three tests were completed at room temperature, where the slower ( $10^{-4}\text{s}^{-1}$ ) strain rate showed a maximum fracture strain of 4.5% and the faster ( $10^{-1}\text{s}^{-1}$ ) strain rate had a value at approximately 13.5%. The maximum stress level reached was roughly 850MPa for the fast tensile test and the slow had a maximum of 800MPa. More specific values of ultimate tensile strength – UTS, offset yield strength  $R_{p0.2}$ , strain hardening ratio and plastic deformation [%] for  $+20^{\circ}\text{C}$  can be seen at Figure 17 and table 3.

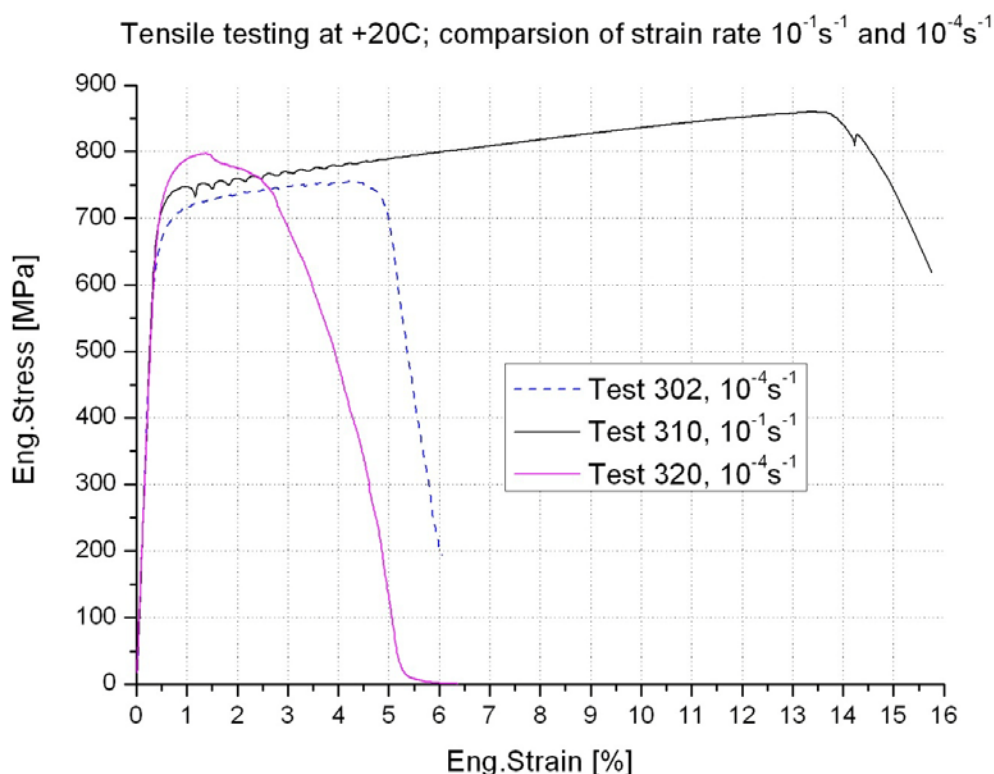


Figure 17. Tensile testing at  $20^{\circ}\text{C}$ , with different strain rates.

Table 3. Comparison of UTS,  $R_{p0.2}$ , strain hardening ratio and plastic elongation at  $+20^{\circ}\text{C}$  tensile testing.

Test number	Strain rate	UTS [MPa]	$R_{p0.2}$ [MPa]	Strain hardening ratio	Plastic elongation [%] (Between $R_{p0.2}$ to UTS)
302	$10^{-4}\text{s}^{-1}$	755	678	1.11 (77)	4.2-0.5=3.7
310	$10^{-1}\text{s}^{-1}$	859	723	1.19 (136)	13.4-0.6=12.8
320	$10^{-4}\text{s}^{-1}$	797	745	1.07 (52)	1.4-0.5=0.9

Two tests were made at the temperature +100°C, where the slow and fast stress/strain curve kept the same shape. The slow could resist up to 10% strain and a stress level over 800MPa. The fast could resist higher strain up to 13% and a stress level of almost 830MPa. Look at Figure 18 and Table 4 for UTS, Rp0.2, strain hardening ratio and plastic deformation valid for the comparison at +100°C.

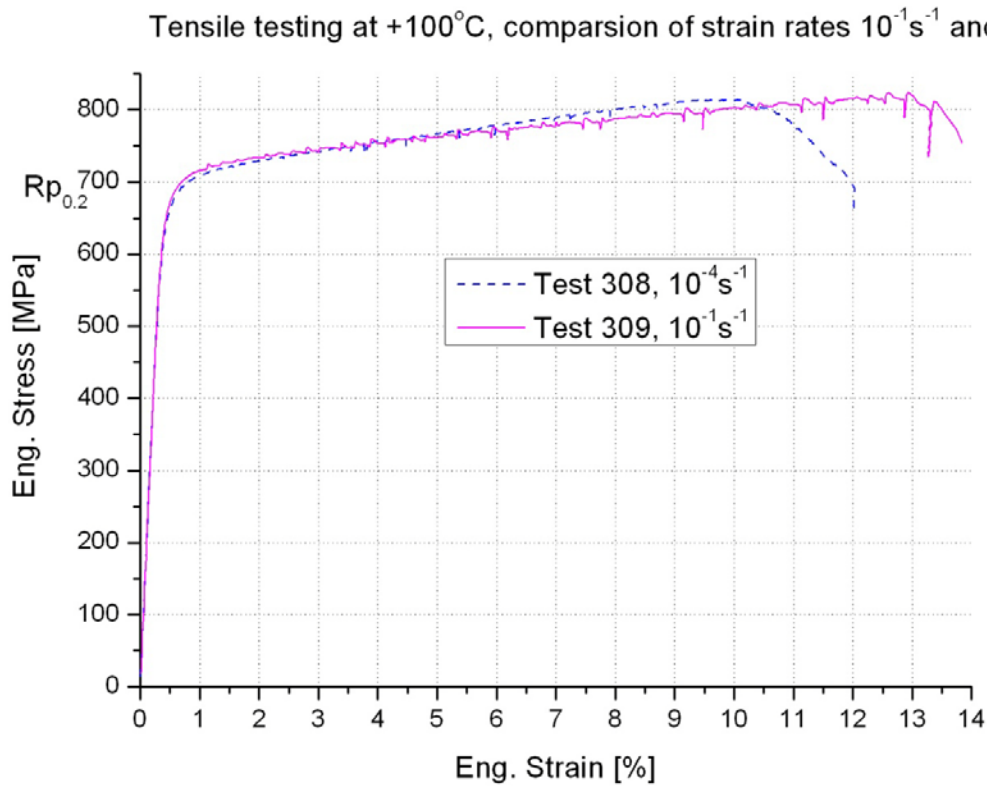


Figure 18. Tensile testing at 100°C, with different strain rates.

Table 4. Comparison of UTS, Rp0.2 and plastic elongation at +100°C tensile testing.

Test number	Strain rate	UTS [MPa]	$R_{p0.2}$ [MPa]	Strain hardening ratio [MPa]	Plastic elongation [%] (Between $R_{p0.2}$ to UTS)
308	$10^{-4}\text{s}^{-1}$	815	674	1.21 (141)	10-0.6=9.4
309	$10^{-1}\text{s}^{-1}$	824	683	1.21 (141)	12.9-0.6=12.3

Two tests were made at the temperature  $-60^{\circ}\text{C}$ , where the faster test showed a bit different curve compare the other tests. The fast one did break earlier than the slower one, with a strain level on 2.5% and stress level on 780MPa. The slow one had a longer strain level up to 4.5% and stress 750MPa until break. See Figure 19 and comparison of UTS, Rp0.2, strain hardening ratio and plastic deformation in table 5.

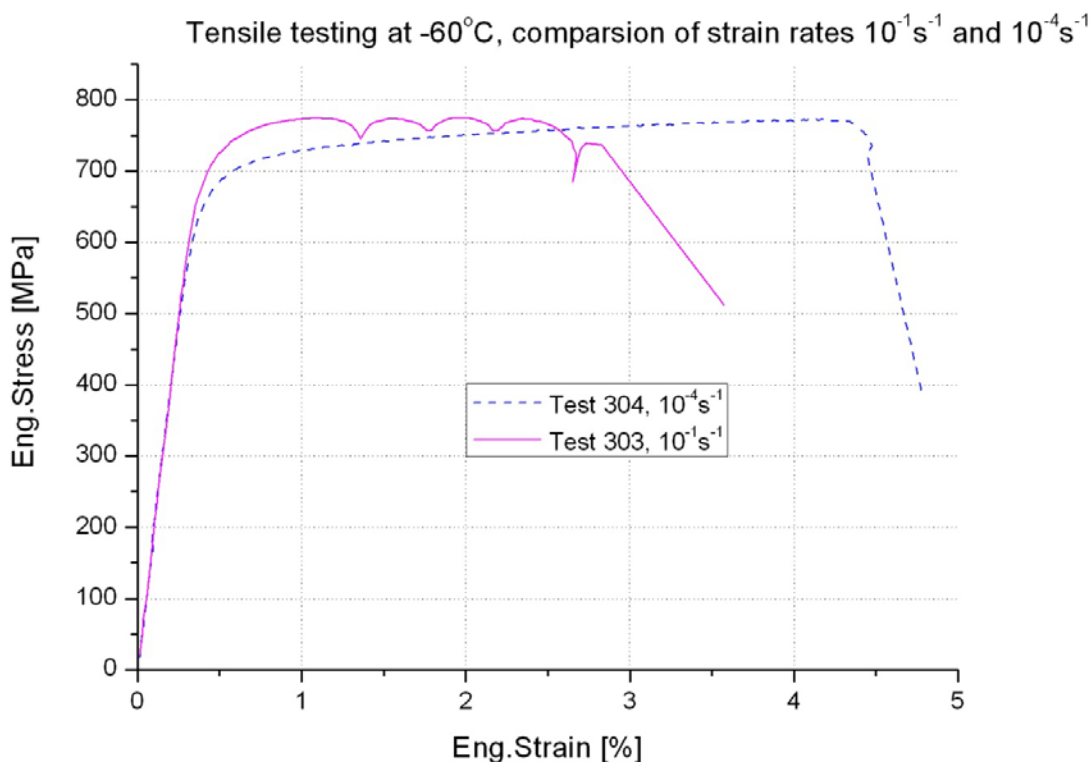


Figure 19. Tensile testing at  $-60^{\circ}\text{C}$ , with different strain rates.

Table 5. Comparison of UTS,  $R_{p0.2}$ , strain hardening ratio and plastic elongation at  $-60^{\circ}\text{C}$  tensile testing.

Test number	Strain rate	UTS [MPa]	$R_{p0.2}$ [MPa]	Strain hardening ratio [MPa]	Plastic elongation [%] (Between $R_{p0.2}$ to UTS)
304	$10^{-4}\text{s}^{-1}$	773	689	1.12 (84)	4.0-0.5=3.5
303	$10^{-1}\text{s}^{-1}$	775	742	1.04 (33)	2.0-0.6=1.4

The different strain rates did not influence the E-modulus (slope of the curve) and the UTS at the same temperature either; mostly the faster test could resist more strain. The higher strain rate in general showed a higher value of stress and fracture strain. Also, higher temperature gave higher fracture strains, possibly indicating reduced defect sensitivity at higher temperatures (also achieved locally due to energy dissipation following plastic deformation).

The plastic deformation in the samples differed a lot and the reason for the variety in the results could be complexity to make homogeneous samples when casting. The largest difference in plastic deformation between identical tests was seen at room temperature, but this can be due to the defect distribution in each individual specimen.

The plastic part of the curves showed a rather linear hardening and a quite short elongation. Fracture strength (UTS) was quite high between 750-900 MPa and it showed that the three different temperatures did not much affect the behaviour of the material.

#### *Comparison with non-EDH Mn13 steel*

The austenitic material is a ductile material in as-cast condition. The fractures in Mn13 EDH material showed an intergranular failure mode due to weak grain boundaries. This was also observed in the as-cast material. The reason for the decreased elongation in the Mn13 EDH compared to the as cast Mn13 could be that the grains have become harder due to the hardening, giving less formability of individual grains and thereby more stressed grain boundaries. A lot of pores and weak layers (sometimes oxidised) were seen at the fracture surface, and the cracks followed the grain boundaries outlining the grains.

The fracture strain values were much lower in the Mn13 EDH material (differ between 1-15% mainly depending on defects) than in as-cast Mn13-steel (~35% at room temperature, ~20-25% at -60°C and ~15-20% at +100°C) and the strain hardening ratio during tensile testing thereby became much lower for Mn13EDH (between 1.04-1.19) than for as-cast Mn13-steel (between 1.72-2.53).

The yield strength in the EDH material is approximately 600MPa while the as-cast material had yield strength around 400 MPa. Neither of the materials showed necking during testing. Resisting of necking is a result of the spread of strain over the whole testing area.

## **5.5 Fatigue testing**

Fatigue testing was made in with both strain- and stress controlled loading. The explosion deformed Mn-steel was around 30% harder than the as-cast Mn-steel. Due to the harder material there were also some difficulties with the fatigue testing with sliding in the grips and of the extensometer. After corrective actions, this could be avoided. The tests presented in the result graphs below, are taken from tests where only the material deficiencies are causing the scatter (except for one test which had overloads every 100 cycles, see comments below).

#### *Strain controlled*

Strain controlled fatigue testing was performed with two tests at each strain amplitude level for 0.3, 0.4, 0.6 and 1%. The 0.3% was an extra level of strain amplitude, introduced because the material could not resist 1% and fractured within a few cycles. The results of the strain controlled testing had large varieties in both lifetime and stress measured. Every curve was first increasing and then decreasing besides for one strength test at level 0.3% (Sample 332). See Figure 20 and a closer look at Figure 21.

A comparison of a maximum reached stress level during the tests at each different strain level resulted in 0.3% ~540MPa, at 0.4% >600MPa, at 0.6% ~750MPa and at 1% >800MPa. Look at Figure 20 and Figure 21.

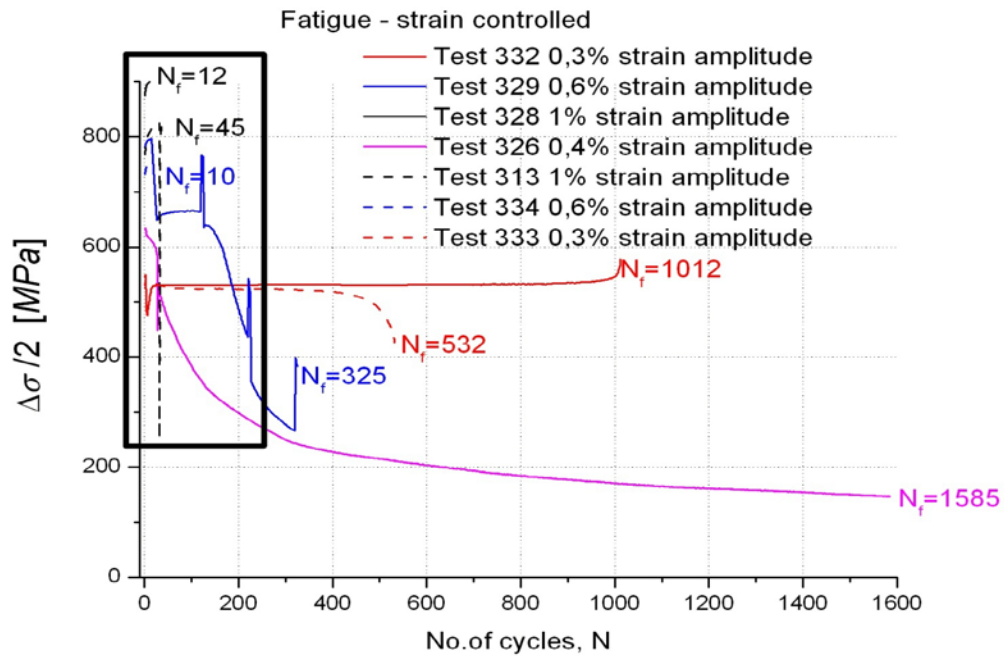


Figure 20. Strain controlled tests. Stress measured vs. number of cycles.

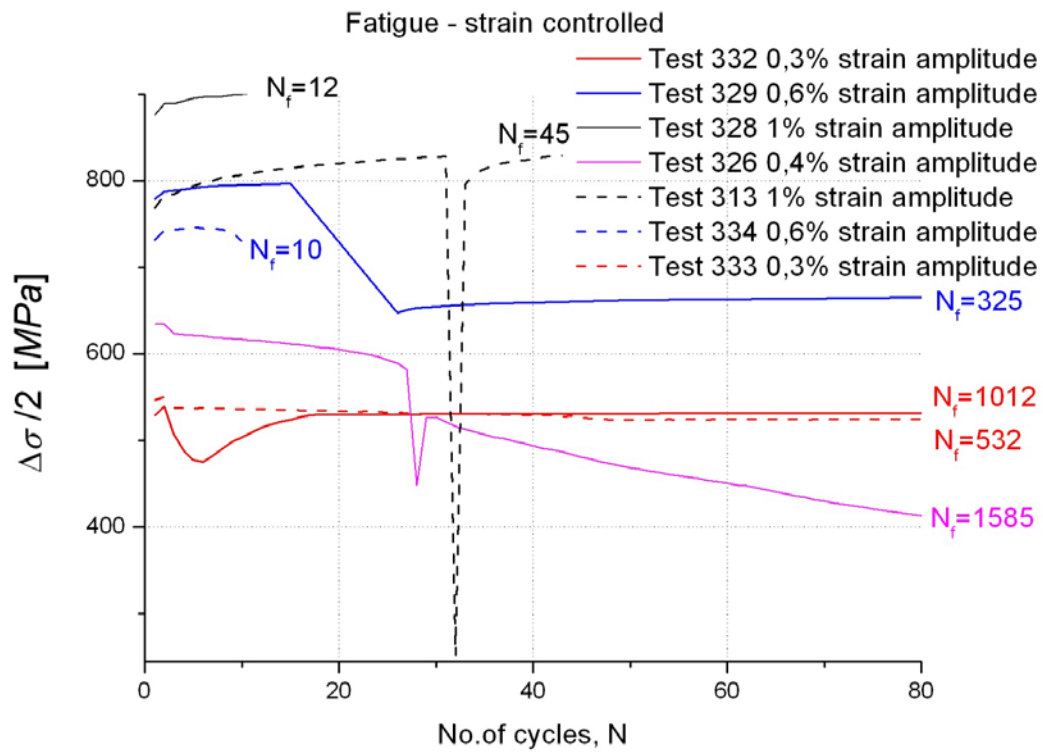


Figure 21. Strain controlled tests, enlargement of figure 20.

The fatigue lifetime in Mn13EDH was lower than for other rail materials; all the samples broke within less than 1600 cycles and the number of cycles to failure was lower than for as-cast Mn-steel.

The scattering of the fatigue lifetime and stress amplitudes can be due to different cast material structures in the samples. The scatter becomes pronounced due to the weak grain boundaries, which cause stepwise crack propagation. Because of the difficulty to distinguish stress amplitude variations due to internal softening from unloading on crack propagation, it is difficult to draw any conclusions regarding the stress amplitude development depicted in Figures 20–21. One of the tests (329) was run with five overloads every 100 cycle (starting with cycle 25), which explains the peaks in the stress amplitude curve and the following dip (probably due to pronounced crack growth during the overload cycles). Despite this higher loading it survived much longer than the other sample run at 0.6% total strain amplitude.

The plastic strain in each cycle became smaller than in the as-cast Mn13 steel due to the higher strength of the Mn13 EDH material. A comparison of the different strain amplitudes can be seen in the hysteresis loops at Figure 22.

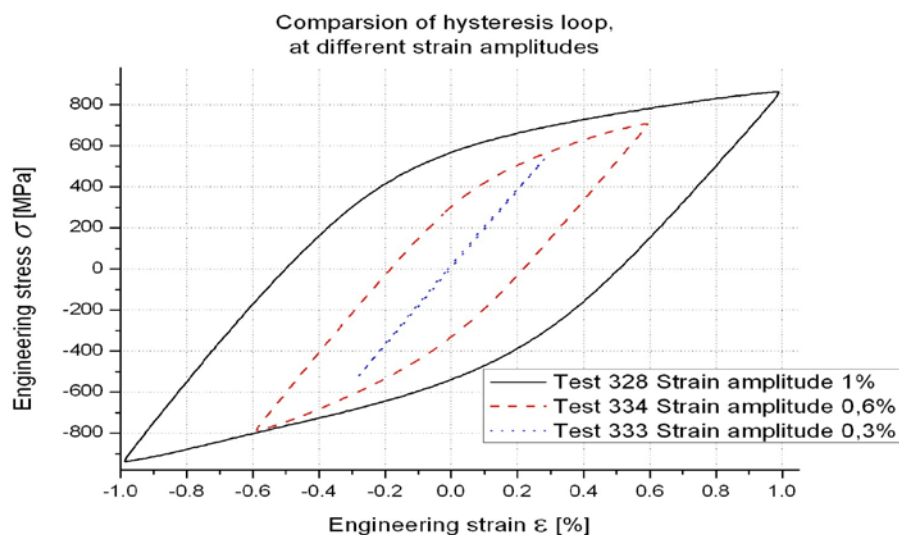


Figure 22. Hysteresis loops for strain level 1%, 0.6 %, and 0.3%

### *Stress controlled*

The maximum levels of stress amplitudes chosen for stress controlled tests were transferred from the maximum stress levels recorded in strain controlled tests. The levels used for stress controlled measuring was 506 MPa (~25kN; ~0.3%), 650MPa (~32kN; ~0.4%), 780MPa (~38.5kN; ~0.6%) and 840MPa (~42kN; ~1%). See Figure 23.

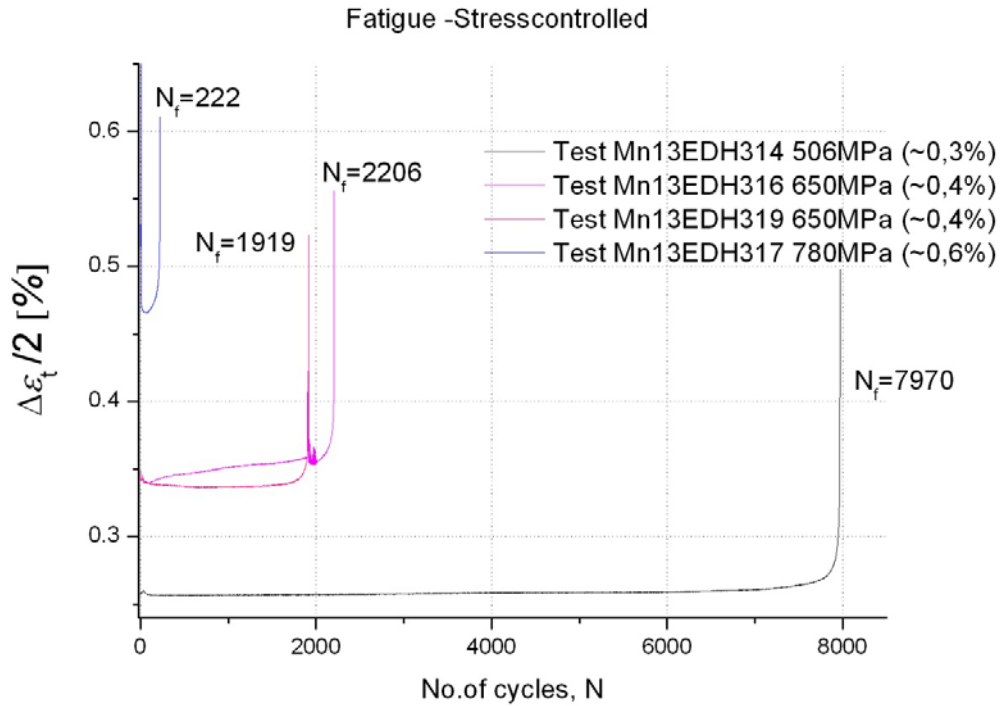


Figure 23. Stress controlled tests. Strain was measured vs. number of cycles.

The curves at Figure 23 showed that the material first hardens (seen as the decreasing first part of the curves), stabilise at values lower than the strain amplitude aimed for. Towards the end of the test, cracks grow larger giving “softening” of the test bar finally leading to failure. Due to the different stress levels used in strain and stress controlled tests; the results were not directly comparable. Also in the stress controlled tests we can expect large influence of defects on strain amplitude development and fatigue life.

A comparison of the hysteresis loops at different strain amplitudes can be seen in Figure 24. The strain axis is to be seen as a relative scale and does not correspond to actual strains.

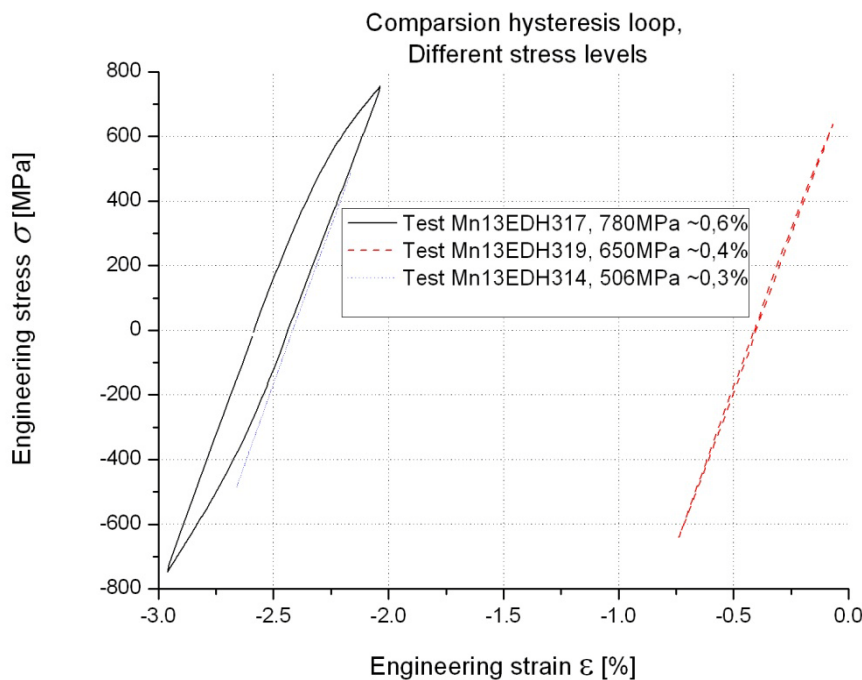


Figure 24. Comparison of hysteresis loops, different stress levels and relative strain axis markings.

## 5.6 Fracture surfaces

The fracture surface of the specimens varied a lot, due to different defects in the material like pores, surface defects like scratches, pores or slags. However, intergranular crack propagation was dominating and the individual grains could be seen. Also cracks along the testing direction could be seen. To see some fracture surfaces and defects look at Figure 25, Figure 26, Figure 27 and Figure 28.

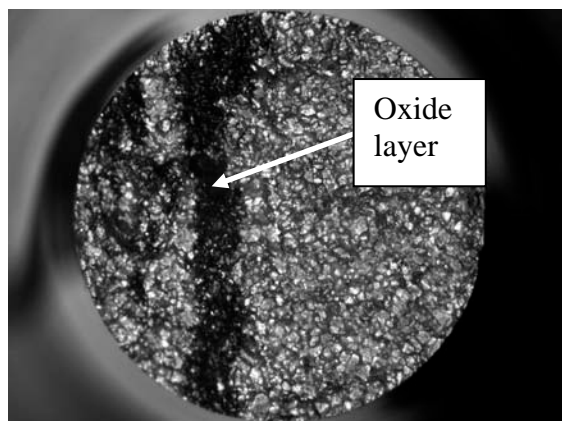


Figure 25. Sample 334 – dark part - oxide layer

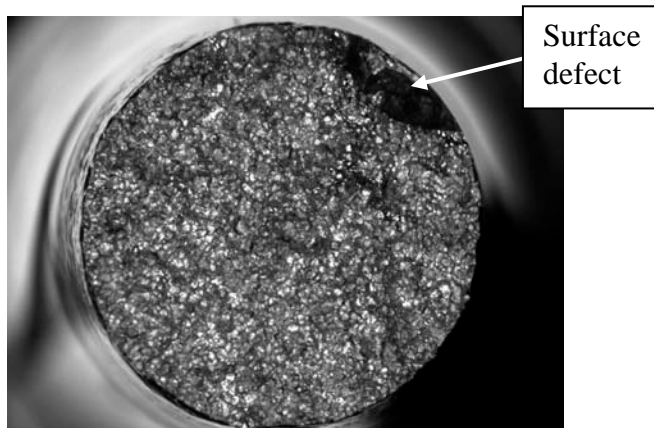


Figure 26. Sample 320 – dark part - surface defect

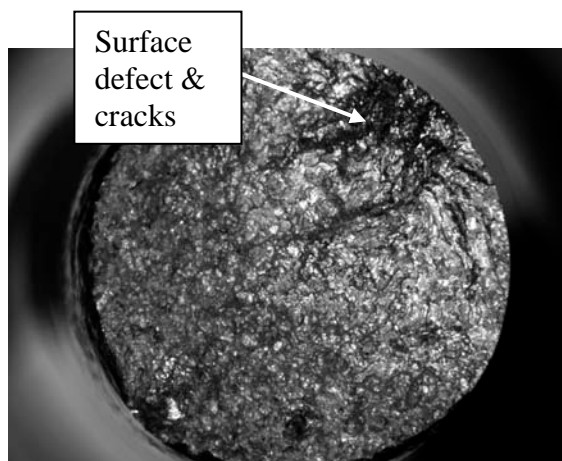


Figure 27. Sample 318 - Surface defects and cracking

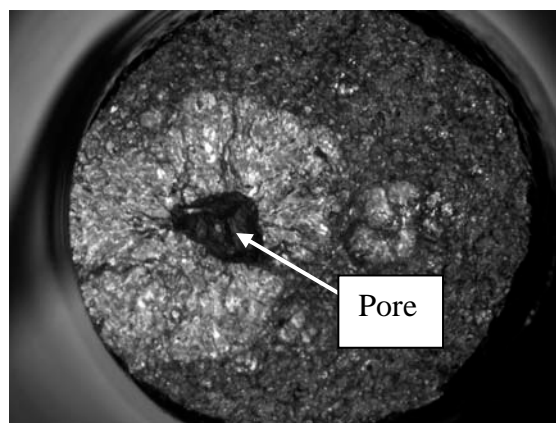


Figure 28. Sample 316 – dark part - Pore

Stresses in combination with defects made the material start cracking, growing and finally break. The outcome was checked with stereo microscopy and dark areas seen on the pictures are the starting point of the crack. The defects weaken the material, gave a shorter fatigue life and lower ductility compared to a more homogeneous material.

## **6. Discussion**

### **6.1 Radiography**

At the fracture surface a lot of small pores and inclusions could be seen, which were not seen on X-ray before mechanical testing. One reason for the difficulty to detect these defects could be that they follow the weak grain boundaries and thus do not lie within one single plane. Radiography was only done at two different angles because of time and cost reasons. Possibly more defects could have been found if more angles would have been tested.

### **6.2 Tensile and fatigue testing**

Since the sample diameter was changed from 6mm to 8mm to avoid buckling in this thesis and the grip diameter was not changed, there became some problems with sliding in the grips of the machine. Also the hard material made it more difficult to fasten and test.

The least precise part of the test is when the operator measures the diameter of the test bar before the test. This can give some percent scatter in measured stress levels, and thus does not explain the large scatter observed in this work.

In this thesis some errors came during the testing for example sliding in the grips, programme fault, extensometer sliding due to unsharp blades etc. These errors typically give unloading of the specimen or extensometer, causing a discontinuity (“jump”) in the recorded data. Such tests have not been included in the result’s section but can be seen in Appendix 1.

The explanation of the scattering of the results in this case is mainly due to the manufacturing methods; casting or the hardening method EDH. The Mn13 type materials are known to be difficult to cast. The EDH treatment increases the defect sensitivity. The material properties are the reason for most of the scatter in the results.

Normally the ductile austenitic Mn13-steel hardens during fatigue loads, but since the material was hardened by explosion depth hardening, the material started on a higher level of hardness. There was over 30% difference in stress amplitude in the first cycles between as-cast and explosive depth hardened manganese steel.

In railway applications, the material is not exposed to high tensile loads which induce and propagate cracks. The repeated compressive loads make it possible to benefit from the high ductility of the individual grains and the thereby high strain hardening of the material. The LCF test is not an ideal method to examine the mechanical behaviour of this material in the application.

## 7. Conclusions

In order to find out mechanical properties and microstructure of the austenitic steel with 13% of Mn, exposed to explosion depth hardening (EDH) tensile, hardness and low cycle fatigue testing was made. The tensile testing was completed at different temperatures and strain rates. The uniaxial push-pull low cycle fatigue testing was controlled both with constant strain- or stress amplitudes.

The major conclusions were:

- Tensile testing at the different temperatures gave limited effects on the mechanical properties like yield strength and ultimate tensile strength - UTS.
- Both for tensile testing in room and at elevated temperatures, the higher strain rate did withstand more strain before fracture (ca 15%). But at lower temperature the specimens tested at high strain rate showed a smaller fracture strain (ca 5%). Yield strength did not differ significantly between tests at different strain rates.
- The yield point for all tests differed between 670-750 MPa, considerably higher than for as-cast Mn13 (~400MPa).
- The strain-hardening was less in the Mn13EDH than as-casted Mn13-steel since the EDH treatment made the material start on a higher hardness level.
- The hardening method through explosion depth hardening, made the material hard with an average hardness of approximately 315HV. Mn13EDH had a smaller number of cycles to failure during low cycle fatigue and resist cyclic deformation worse than as-cast Mn13-steel. All the fracture surfaces showed an intergranular failure.
- The samples had a lot of small pores and defects and the number of cycles to failure scattered a lot between different specimens.
- Both strain and stress controlled tests showed rather constant strain levels throughout the test, independent on what level of stresses were tested. This is very different from the as-cast Mn13 steel which hardens up to 50% during the initial part of the test. However, the loss of this additional hardening is thought to be a consequence of cracks, as the performance in field of Mn13 EDH is very good.
- Low cycle fatigue test results regarding number of cycles to failure are not representative for the material behaviour in the application. The reason is the high tensile loads in the tests causing cracks thereby leading to premature failure.

## References

- Ahlström, J. (2009). *Lecture notes from Failure Analysis course*. Göteborg, Sweden: Chalmers University of Technology at Materials and Manufacturing Department.
- Andersson, E., & Berg, M. (2007). *Spårtrafiksystem och spårfordon, Del 1: Spårtrafikssystem*. Stockholm: Järnväggruppen KTH.
- ASM Handbook online, v. 8. (2003). Fatigue and Fracture Mechanics.
- Callister, W. D. (1997). *Materials Science and Engineering - An introduction* (4 uppl.). Canada, USA: John Wiley & Sons, Inc.
- Dieter, G. E. (2003). Mechanical Behavior Under Tensile and Compressive Loads, ASM Handbook online vol. 8.
- Efstathiou, C., & Sehitoglu, H. (2009). Strain hardening and heterogeneous deformation during twinning in Hadfield steel. *Acta Materialia Inc.no 58 / ScienceDirect*, 1479-1488.
- Fatigue and Fracture Mechanics, ASM Handbook online vol.8. (2003).
- George, F., & Voort, V. (2003). Microindentation Hardness Testing, ASM Handbook online vol. 8.
- Hammar, L. (2010, 03 17). X-ray results of MN13 EDH. (L. Norberg, Interviewer) <http://www.gordonengland.co.uk/hardness/vickers.htm>. (n.d.). Retrieved 2010.08.20
- <http://www.voestalpine.com>. (n.d.). (Voestalpine, VAE) Retrieved 2010.03.01, from [http://www.voestalpine.com/vae/en/products/railway\\_infrastructure/switchsystems.html](http://www.voestalpine.com/vae/en/products/railway_infrastructure/switchsystems.html).
- Krahl, P. (2007). Fatigue properties of Martensitic Steel for Use in Highly Stressed Railway Components. Göteborg, Sweden: Chalmers University of Technology.
- Lewis, R., & Olofsson, U. (2009). *Wheel-rail interface handbook* (Vol. 2). North America, USA: CRC Press LLC.
- Österberg, S. (September 2007). Fatigue properties of austenitic Mn-steel for use in highly stressed railway components. Göteborg: Chalmers University of Technology.
- Revanker, G. (2003). Introduction to Hardness Testing, ASM handbook online vol. 8.
- Schilke, M. (2010). , Personal communication.
- Tobolski, E. L., & Fee, A. (2003). Macroindentation Hardness Testing, ASM Handbook online vol. 8.
- Todd, M. (u.d.). ASM Handbook Volume 8, Mechanical Testining and Evaluation.
- Ullman, E. (1997). *Karlebo, Materialteknik* (13 uppl.). Värnamo, Sverige: Fählths Tryckeri AB (printing house).
- Zuidema, B., Subramanyam, D., & Leslie, W. (09 1987). The effect of Aluminium on the work hardening and wear resistance of hadfield manganese steel. *Metallurgical Transitions A*, 18A, ss. 1629-1639.

Appendix 1

Marking No.	Plate	Fatigue testing		Tensile testing		Amplitude [%/kN/MPa]	Strain/stress after half lifetime [MPa/% @ NF/2]	Plastic strain amplitude [Ep @ NF/2] [%]	No. of cycles to failure (Life time) [NF]	Problems/ Ratcheting	r after grinding with 1200 (final- tensile) [φ in mm]
		Stress controlled [σ in MPa]	Strain controlled [ε in %]	Slow 0.0001 [+20°C]	Fast 0.1 [+20°C]						
301	C/D (1 <sup>st</sup> )	*	*								
302	C/D (1 <sup>st</sup> )	*	*							Programme failure, grip scratches. Ends pushed together.	7.94
303	C/D (1 <sup>st</sup> )	*	*							Grip scratching.	7.95
304	C/D (1 <sup>st</sup> )	*	*								7.93
305	C/D (1 <sup>st</sup> )	*	*							Programme failure	7.93
306	C/D (1 <sup>st</sup> )	*	*							Fail under extenso.	7.94
307	C/D (1 <sup>st</sup> )	*	X			0.4%	W	W	W	Take to stresscont!	7.96
308	C/D (1 <sup>st</sup> )	*	*								7.95
309	C/D (1 <sup>st</sup> )	*	*								7.96
310	C/D (1 <sup>st</sup> )	*	*								7.93
311	C/D (1 <sup>st</sup> )	*	*							Fail under extenso.	7.95
312	C/D (1 <sup>st</sup> )	*	X			0.40%	W	W	W	Too high load. Limitation stopped 43kN	7.94
313	A/B (2 <sup>nd</sup> )	*	X			1.00%	821.09	0.534	45	Sliding, restart, fail under ext.	7.93
314	A/B (2 <sup>nd</sup> )	X	(~0.3%)			25kN/506MPa	0.2584	0.000555	7970	One missed rubber. Little plastic def.	7.94
315	A/B (2 <sup>nd</sup> )	X	(~0.6%)			38.5kN/780MPa	W	W	W	Sliding many times. Stopped.	7.93
316	A/B (2 <sup>nd</sup> )	X	(~0.4%)			32.1kN/650MPa	0.3519	0.0116	2206	Fail under extenso.	7.94
317	A/B (2 <sup>nd</sup> )	X	(~0.6%)			38.5kN/780MPa	0.468	0.0735	222	Slid, paused, fail under extenso.	7.94
318	A/B (2 <sup>nd</sup> )	X	(~0.3%)			25.1kN/506MPa	?	0.00381	6576		7.95
319	A/B (2 <sup>nd</sup> )	X	(~0.4%)			32.2kN/650MPa	0.037	0.005	1919	Sliding 7 times. Tried rubber -> bad.	7.95
320	A/B (2 <sup>nd</sup> )	*	*								7.95
321	A/B (2 <sup>nd</sup> )	*	*								7.95
322	A/B (2 <sup>nd</sup> )										7.96
323	A/B (2 <sup>nd</sup> )										7.96
324	A/B (2 <sup>nd</sup> )										7.96
325	A/B (2 <sup>nd</sup> )	*	X			1%/32kN max	885.35	0.476	2	Test if buckling on dia.7mm, No polish	*
326	A/B (2 <sup>nd</sup> )	*	X			0.4%/25kN max	185	0.0096	1585	Fast cracking, long to failure	7.00
327	A/B (2 <sup>nd</sup> )	*	X			0.30%	646.67	0.00967	3237	Crack 1500 cycles. Continue to fail.	6.36
328	A/B (2 <sup>nd</sup> )	*	X			1%/32kN max	896.47	0.499	12	Fail under extenso.	7.00
329	A/B (2 <sup>nd</sup> )	*	X			0.6%/30kN max	604.32	0.197	325	Variable segments-missed.	7.00
330	A/B (2 <sup>nd</sup> )	X	(~1%)			32.2kN/(840MPa)	W	W	<1 cycle	Fail over extenso. Turned specimen.	6.99
331	A/B (2 <sup>nd</sup> )	*	X			0.40%	W	W	W	Slid. Not tested properly	6.98
332	C/D (2 <sup>nd</sup> )	*	X			0.30%	~531.5	0.0033	1012	Fail under extensometer.	7.03
333	C/D (2 <sup>nd</sup> )	*	X			0.30%	523.6	0.00932	532		7.03
334	C/D (2 <sup>nd</sup> )	*	X			0.60%	745.91	0.199	10 ? 71/2?		7.06
335	C/D (2 <sup>nd</sup> )										7.03
336	C/D (2 <sup>nd</sup> )										7.03
337	C/D (2 <sup>nd</sup> )										7.00

?= Can not get values through Matlab programme. Something is wrong, raw no.  
W = something went wrong with the test. Not tested to failure